Iranian Journal of Basic Medical Sciences
ijbms.mums.ac.ir

Enhanced effects of Wharton's jelly–derived MSC secretome and microbial exopolysaccharide on cellular responses and tissue repair in diabetic wound healing

Hossein Rostami [1], Seyed Mohamad Amin Haramshahi [2, 3], Nasim Vousooghi [1], Somayeh Shamlou [1], Zeinab Shahmahmoudi [2, 3], Peiman Brouki Milan [2, 3]*, Javad Verdi [1]*

[1] Department of Applied Cell Sciences, School of Advanced Technologies in Medicine, Tehran University of Medical Sciences, Tehran, Iran
[2] Department of Tissue Engineering and Regenerative Medicine, Faculty of Advanced Technologies in Medicine, Iran University of Medical Sciences, Tehran, Iran
[3] Cellular and Molecular Research Center, Iran University of Medical Sciences, Tehran, Iran

ARTICLE INFO

Article type:
Original

Article history:
Received: May 13, 2026
Accepted: Jul 21, 2026

Keywords:
Diabetes mellitus
Wound healing
Mesenchymal stem cells
Secretome
Fibroblasts
Endothelial cells
Exopolysaccharide

ABSTRACT

Objective(s): Diabetic wounds are characterized by impaired healing and chronic inflammation. This study evaluated a combination therapy using an exopolysaccharide derived from *Rhodotorula mucilaginosa* sp. GUMS16 (EPS-GUMS16) and Wharton's jelly-derived mesenchymal stem cell-conditioned medium (WCM) to accelerate wound repair.

Materials and Methods: Human foreskin fibroblasts (HFFs) and human umbilical vein endothelial cells (HUVECs) were treated with an optimized concentration of the WCM/EPS-GUMS16 (WCM/EPS) combination. *In vitro* assays, including MTT and scratch wound assays, were conducted to assess cell proliferation and migration. *In vivo*, full-thickness wounds in diabetic rats were treated with WCM/EPS via subcutaneous injection and topical application. Wound healing was monitored by measuring the reduction in wound surface area, and histopathological evaluation was performed using hematoxylin and eosin (H&E) and Masson's trichrome (MT) staining.

Results: *In vitro* assessments showed that WCM/EPS enhanced fibroblast proliferation and migration ($P<0.05$) and significantly upregulated CDK-4 expression ($P<0.05$). *In vivo*, treated wounds exhibited increased epidermal thickness and altered blood vessel density compared with controls. Semi-quantitative histopathological analysis further revealed enhanced re-epithelialization, more organized granulation tissue, and reduced inflammation and edema. These findings indicate that WCM/EPS effectively modulates inflammation and angiogenesis, thereby promoting tissue regeneration in diabetic wounds.

Conclusion: Overall, this combination is a promising strategy for improving diabetic wound healing and highlights the potential of integrating microbial exopolysaccharides with stem cell-derived conditioned media in regenerative therapies.

▶ Please cite this article as:
Rostami H, Haramshahi SMA, Vousooghi N, Shamlou S, Shahmahmoudi Z, Brouki Milan P, Verdi J. Enhanced effects of Wharton's jelly–derived MSC secretome and microbial exopolysaccharide on cellular responses and tissue repair in diabetic wound healing. Iran J Basic Med Sci 2026; 29:

Corrected Proof

Introduction

Diabetic patients suffer from many complications, but the most common and costly complication is diabetic foot ulcer (DFU). More than 80% of lower limb amputations in patients with diabetes are associated with DFU (1). Hyperglycemia, chronic inflammation, and hypoxia are among the factors that affect the wound healing process in diabetic patients (2). Chronic DFUs often remain in the inflammatory phase and do not undergo the normal wound-healing process. This is caused by the release of pro-inflammatory molecules, elevated reactive oxygen species levels, and impaired re-epithelialization of the wound bed (2, 3). Currently, the standard care and management of DFUs encompass pressure alleviation, debridement of necrotic tissue, infection control, and restoration of vascular perfusion. However, a considerable proportion of chronic DFUs are resistant to these standard therapeutic approaches and remain unhealed. In recent years, investigators have examined the effectiveness of adjuvant therapies, bioengineered skin substitutes, growth factors, and cell therapy for treating DFUs to develop more effective therapeutic approaches (4, 5). In addition, a significant body of research has focused on identifying effective, affordable, and readily available therapies that leverage natural substances and composites (6). One such class of compounds is exopolysaccharides (EPSs), which are produced by bacteria, fungi, and algae (7). Hamidi *et al.* were the first to extract and characterize the exopolysaccharide produced by a cold-adapted yeast strain,

**Corresponding authors:* Peiman Brouki Milan. Department of Tissue Engineering and Regenerative Medicine, Faculty of Advanced Technologies in Medicine, Iran University of Medical Sciences, Tehran, Iran. Email: Peiman.brouki@gmail.com, Brouki.p@iums.ac.ir; Javad Verdi: Department of Applied Cell Sciences, School of Advanced Technologies in Medicine, Tehran University of Medical Sciences, Tehran, Iran. Email: j-verdi@sina.tums.ac.ir

© 2026. This work is openly licensed via CC BY 4.0.
This is an Open Access article distributed under the terms of the Creative Commons Attribution License (https://creativecommons.org/licenses), which permits unrestricted use, distribution, and reproduction in any medium, provided the original work is properly cited.

Rhodotorula mucilaginosa sp. GUMS16 (EPS-GUMS16). They demonstrated the biocompatibility and antioxidant properties of EPS-GUMS16 (8). In a subsequent study, Hivechi *et al*. evaluated EPS-GUMS16 in combination with PCL/Gel nanofibers for the treatment of incisional wounds in a rat model. The results indicated that treatment with the PCL/Gel and EPS combination accelerated wound healing. Furthermore, the results revealed increased granulation tissue formation, accompanied by a higher number of fibroblasts and microvessels surrounding the wound site, likely owing to the antioxidant and anti-inflammatory properties of EPS (9). Its antioxidant activity is attributed to the presence of mannose in its structure (8). In contrast, its anti-inflammatory activity is likely mediated, as with many polysaccharides, by inhibition of the MAPK/NF-κB signaling pathway (10). Concurrent with the investigation of natural compounds, the use of mesenchymal stem cells (MSCs) and their derivatives, particularly conditioned media, has attracted considerable attention in the scientific community. A substantial body of research has demonstrated the beneficial effects of these cellular products in promoting diabetic wound healing. Conditioned medium (CM) contains a broad spectrum of extracellular vesicles (EVs), cytokines, growth factors, and other bioactive molecules secreted by cells (11). Research in this field has demonstrated that MSCs-derived conditioned medium (MSCs-CM), which contains bioactive factors such as VEGF, PDGF, TGF-β, FGF-2, HGF, IL-10, SDF-1, PGE2, and IL-6 (12) exerts multifaceted effects on diabetic wound healing through mechanisms including immunomodulation, angiogenesis, and the stimulation of proliferation and migration of key cell types, such as keratinocytes and fibroblasts (13-16). Considering the antioxidant effects of EPS-GUMS16 and the immunomodulatory effects of MSCs-CM, it seems that using the combination of Wharton's jelly-derived mesenchymal stem cell-conditioned medium (WCM) and exopolysaccharide derived from *R. mucilaginosa* sp. GUMS16 (EPS-GUMS16) may enhance therapeutic effects by facilitating the transition from the inflammatory phase and accelerating the healing process in diabetic wounds. Despite previous studies on EPS-GUMS16, the precise mechanisms by which it promotes wound healing, particularly in diabetic wounds, remain unclear. In the present study, we adopted an innovative approach to investigate the enhanced therapeutic effects of EPS-GUMS16 and WCM on diabetic wound healing. We also investigated the combined effects of EPS and WCM on fibroblasts and human umbilical vein endothelial cells (HUVECs) to elucidate the mechanisms underlying their promotion of diabetic wound healing.

Matrials and Methods

Materials

Phosphate-buffered saline (PBS), ammonium sulfate, glycerol, Potato Dextrose Broth (PDB) medium, 3-[4.5 dimethylthiazol- 2-yl]-2.5-diphenyltetrazolium bromide (MTT), ketamine, xylazine, streptozotocin (STZ), and sucrose were purchased from Sigma Aldrich (Sigma Aldrich Co, USA). HCl, ethanol 96%, penicillin/streptomycin (pen/strep), and dimethyl sulfoxide (DMSO) were obtained from Merck (Darmstadt, Germany). Dulbecco's Modified Eagle Medium-F12 and fetal bovine serum (FBS) were purchased from Gibco (Gibco BRL Ltd, Paisley, Scotland), and the TriZol reagent and cDNA synthesis kit were obtained from Thermo Fisher (Thermo Fisher Co., USA).

Cell isolation and culture

Human foreskin fibroblasts (HFFs) and HUVECs were obtained from the Cell Bank of the University of Medical Sciences, Tehran, Iran. Wharton's jelly-derived mesenchymal stem cells (WJ-MSCs) were isolated from umbilical cord-derived Wharton's jelly. During this study, all cell types were cultured in Dulbecco's Modified Eagle Medium/F12 (DMEM/F12) supplemented with 10% fetal bovine serum (FBS).

WJ-MSCs Isolation, expansion, and characterization

Umbilical cord samples from newborns were obtained with informed consent from the donors. After collection, the umbilical cord was transferred to the laboratory in a sterile container containing PBS solution with 2% Pen/Strep. After proper washing with PBS and separating the blood arteries and veins, Wharton jelly was cut into 2-3 mm2 pieces. These pieces were transferred to 10-cm plates containing DMEM-F12 supplemented with 15% FBS and 1% Pen/Strep, and then incubated in a humidified 5% CO2 atmosphere at 37 °C. Morphological assessment, flow cytometric characterization (CD90, CD73, and CD105 as positive markers and CD45 and CD34 as negative markers), and multilineage differentiation were performed using passage 2 WJ-MSCs. Following characterization, the cells were expanded and cryopreserved at passage 3. For WCM preparation, cryopreserved cells were thawed, re-expanded, and conditioned medium was collected from passage 5 cells.

Preparation of conditioned media (CM)

When the confluency of human WJ-MSCs reached approximately 80%, the medium was replaced with serum-free DMEM/F12. Then, WCM was collected after 48 hr. To remove cell debris, the cell pellet was centrifuged for 5 min at 2000 rpm (Eppendorf centrifuge 5702, Germany). All steps were done under sterile conditions. For the subsequent experiments, the WCM was filtered through a 0.22-µm syringe filter and stored at −80 °C.

EPS-GUMS16 production and isolation

The EPS was isolated according to the method used by Hivechi *et al*. (9). In summary, Potato Dextrose Broth (PDB) medium was used for yeast culture. This culture medium was made using a combination of PDB powder, ammonium sulfate, and sucrose in deionized water. The pH of the medium solution was adjusted to 6 with 1 M HCl, then autoclaved at 121 °C and stored at 4 °C. The isolated *R. mucilaginosa* sp. GUMS16 was cultured in a sterile PDB medium and then incubated for 24 hr at 30 °C. Incubation was then continued at 4 °C for 72 hr. The resulting single colonies were preserved in 30% glycerol as stock for the next steps. The cold-adapted yeast was extracted from the stock, added to PDB medium in Erlenmeyer flasks, and incubated at 25 °C in a shaking incubator at 150 rpm. Afterward, the medium including the yeast was centrifuged for 30 min at 8500 RFC and 4 °C. The supernatant was collected, and the exopolysaccharide was precipitated with ethanol. The supernatant was discarded, and the precipitate was washed with cold ethanol and centrifuged at 8500 RFC for 20 min at 4 °C. The precipitate was rewashed with ethanol and centrifuged as mentioned above. After that, the resulting precipitate was solubilized in deionized water, then

Corrected Proof

incubated at 80 °C overnight, and freeze-dried for 48 hr at 60 °C and 5 mbar.

***In vitro* study**

Ethics statement

All protocols of this research were approved by the Research Ethics Committee of an academic institution (certificate ID: IR.TUMS.AEC.1400.038).

MTT assay

To determine the potential effects of WCM and EPS on cell viability and proliferation, HFFs and HUVECs at a density of 2×03 cells/well were seeded into 96-well plates. After overnight cultivation in DMAM/F12 supplemented with 10% FBS and 1% penicillin/streptomycin, culture media were exchanged with fresh media comprising defined concentrations (Optimized concentrations through viability testing) of WCM (10%), EPS (200µg/ml), and WCM (10%)/EPS (200 µg/ml) combination. After 24 and 48 hr of incubation, the culture medium was replaced with 100 µl PBS solution containing 0.5 mg/ml MTT (3-[4.5 dimethylthiazol- 2-yl]-2.5-diphenyltetrazolium bromide). After that, the plates containing cells were incubated at 37 ˚C, 95% humidity, and 5% CO_2 for 3 hr. Then, to dissolve the dye crystals, the MTT solution was replaced with 100 µl of dimethyl sulfoxide (DMSO). The samples were incubated for 15 min in the dark. Finally, the absorbance of each well was measured at 570 nm by a microplate reader device (Bio-Rad 680, USA).

Scratching assay

The impact of compositions (WCM, EPS, and WCM/EPS) on cell migration was evaluated using an *in vitro* cell migration assay. HFFs and HUVECs were individually seeded on 48-well plates at a density of 2×10^4 cells per well and allowed to reach 80% confluency. After that, a scratch was created at the center of each well using a pipette tip. To remove cell debris, the medium was removed, and the plate was gently washed once with serum-free medium. Finally, the new culture medium containing WCM 10%, EPS 200 µg/ml, and WCM 10%/EPS 200 µg/ml combinations was added to the cells and incubated at 37 °C. Cell migration toward the scratched area was tracked and photographs of the scratch were taken at 0, 12, and 24 hr using an inverted microscope (Carl Zeiss, Germany). The scratch area was measured by ImageJ software.

Gene expression analysis

HFFs and HUVECs were treated for 48 hr with WCM10%, EPS 200µg/ml, and a combination of WCM 10%/EPS 200µg/ml (Optimized concentrations through viability testing). Untreated cells were considered the control group. Total RNA was then extracted using TRIzol reagent. The total RNA was evaluated using a NanoDrop Spectrophotometer (Nabi, MicroDigital Co., Ltd., Korea). RNA quality was evaluated using absorbance ratios at 260/280 and 260/230 nm, and RNA was standardized to 250 ng of total RNA per reaction with nuclease-free water (17).

Reverse transcription was performed using the complementary DNA (cDNA) synthesis kit. The reaction was conducted in a total volume of 20 µl, following the manufacturer's instructions. Supplementary 1 displays the sequences of the forward and reverse primers, specific annealing temperatures, and amplicon sizes. The PCR amplification of the collagen type I, VEGF, and CDK4 genes was performed using a Rotor-Gene 6000 real-time PCR (RT-PCR) machine (Corbett Life Science, Sydney, Australia). The relative mRNA concentrations of the target genes were normalized to GAPDH, the housekeeping gene. The comparative Ct method was used to determine differences for each target gene, and the results were presented as fold changes relative to the control (17).

In vivo study

Type I diabetes induction and evaluation

Adult male 12-week-old Wistar albino rats (200–220 g) were obtained from a certified laboratory animal supplier. Before the experimental procedures, the animals were given a period of adaptation to laboratory conditions. The subjects were granted unrestricted entry to conventional conditions (25 °C, 30-70% humidity, and a 12-hour light:12-hour dark cycle). To induce diabetes, the rats were made diabetic one week before treatment by administering a single intraperitoneal injection of STZ (55 mg/kg body weight). Three days after the STZ injection, blood glucose levels were measured. Rats with blood glucose levels greater than 220 mg/dl were considered diabetic if they maintained high blood glucose for three days.

Wound creation, animal groups, and treatment

The sixteen diabetic rats (n=16) were randomly assigned to four treatment groups (n=4 rats per group), including the control group (treated with DMEM/F12), the WCM group (treated with 10% WCM), the EPS group (treated with 200 µg/ml EPS-GUMS16), and the WCM/EPS group (treated with a combination of 10% WCM and 200 µg/ml EPS-GUMS16).

Diabetic rats in each group were anesthetized with ketamine/xylazine (90/5 mg/kg body weight), and the dorsal hair was removed by shaving. After hair removal, under sterile conditions, two full-thickness wounds measuring 2 × 2 cm were created in the dorsal region of each rat using a scalpel and scissors (18). Both wounds on the same animal received the same treatment throughout the study. The rats received an intramuscular antibiotic injection (10 mg/kg body weight) during the first three days after wound creation to prevent infection.

For all groups, the treatment of each wound consisted of a subcutaneous injection of 100 µl of the designated solution (25 µl at each of the four wound margins) and a topical spray of 50 µl on the wound surface on days 1, 4, and 7 after wound creation.

For histopathological evaluation, two rats from each group were euthanized on day 7 (8 rats in total), while the remaining two rats from each group were euthanized on day 14 (8 rats in total). The remaining animals were followed until day 14 for serial wound-closure assessments.

Macroscopic evaluation of wounds (estimation of wound closure rate)

Wound evaluations, photographs, and measurements were conducted at four time points: 0, 4, 9, and 14 days post-wound creation. The percentage of wound closure was determined by applying the following equation: *wound closure (%)*$=(A_0-A_t)/A_0\times100$, where A_0 represents the wound area at Day 0 and A_t denotes the wound area 4, 9, or 14 days after wound creation. The wound area was measured by ImageJ 1.52v software.

Corrected Proof

Histopathological analysis

Rats were euthanized at 7 (n=8) and 14 (n=8) days after surgery. The skin samples, comprising both the wound region and the surrounding skin, were carefully separated and collected. Afterward, the specimens were fixed in 10% formalin, processed, and embedded in paraffin blocks. Perpendicular serial sections were obtained along the wound axis, and several sections from each sample were prepared on slides for staining with hematoxylin and eosin (H&E) and Masson trichrome (MT). The H&E and MT staining procedures were performed as described by Sheehan and Hrapchak (18). Inflammation, organized granulation tissue, hemorrhage, edema, and re-epithelialization were assessed and qualitatively ranked by the pathologist, who was unaware of the experimental groups. Inflammation was assessed by the extent of inflammatory cell infiltration. Furthermore, the number of vessels and the thickness of the formed epidermis were quantified. The numbers of microvessels, lymphocytes, neutrophils, and macrophages in the microscopic fields were assessed at 400× magnification (Olympus, Japan). In the microscopic evaluation of each investigated parameter, 10 microscopic fields were examined for each sample.

Epidermal thickness measurement

Epidermal thickness was manually assessed on H&E-stained tissue sections using a calibrated light microscope equipped with an ocular micrometer, following the method described by Therkildsen *et al.* (19). Measurements were performed after calibrating the microscope with a stage micrometer. In each sample, five non-overlapping fields with perpendicular orientation to the epidermal surface were selected, while oblique or highly curved areas were excluded to minimize measurement error. Final values were corrected for magnification. The corrected values were used to calculate the mean epidermal thickness and perform statistical comparisons between experimental groups.

Statistical analysis

All data are presented as mean±SD. Statistical analyses were performed using GraphPad Prism version 10.2.3.403. Two-way ANOVA, followed by Tukey's multiple comparisons test, was used to analyze cell viability and the *In vitro* wound-healing (scratch) assay. One-way ANOVA, followed by Dunnett's multiple comparisons test, was used to analyze relative gene expression determined by quantitative real-time PCR (qRT-PCR). Histopathological findings were interpreted descriptively because of the limited number of animals available for histological evaluation at each time point. A 95% confidence interval was used, and $P<0.05$ was considered statistically significant.

Results

The human WJ-MSCs characterization and preparation of WCM

The isolated WJ-MSCs at passage 2 exhibited a spindle-shaped, fibroblast-like morphology (Supplementary 2a) and expressed the surface markers CD73, CD90, and CD105, while lacking the expression of the hematopoietic markers CD34 and CD45. Flow cytometric analysis confirmed the cells were MSCs, with expression of all positive markers exceeding 93% and negative markers remaining below 3% (Supplementary 2b). According to the criteria established by the International Society for Cell & Gene Therapy (ISCT), these surface markers are considered characteristic of MSCs (20). Furthermore, the cells demonstrated the capacity to differentiate into osteocytes and adipocytes (Supplementary 2a). WCM was collected from passage 5 cells and stored at −80 °C, as described in the Materials and Methods section.

EPS Characterization

The FTIR spectrum of the extracted EPS is presented in Supplementary Figure 3. As reported by Hamidi *et al.* (8), the absorption peaks at 3449.04, 1574.95, 1419.06, and 1119.61 cm^{-1} correspond to hydroxyl (–OH), carbonyl (C=O), methylene (CH_2), and S=O or C–O functional groups, respectively.

Cell proliferation and viability assay

The MTT assay demonstrated that, after 48 hr. the viability and proliferation of HFFs and HUVECs treated with WCM were significantly higher than those of the control group (Figure 1A). Overall, treatment with 10% WCM resulted in significantly greater viability and proliferation of both HFFs and HUVECs than treatment with the other concentrations (5% and 20% WCM). Therefore, 10% WCM was selected as the optimal concentration for subsequent *in vitro* and *in vivo* experiments. The MTT assay performed after 48 hr also revealed significant differences in the proliferation of HFFs and HUVECs following treatment with four different concentrations of EPS (100–800 µg/ml) compared with the

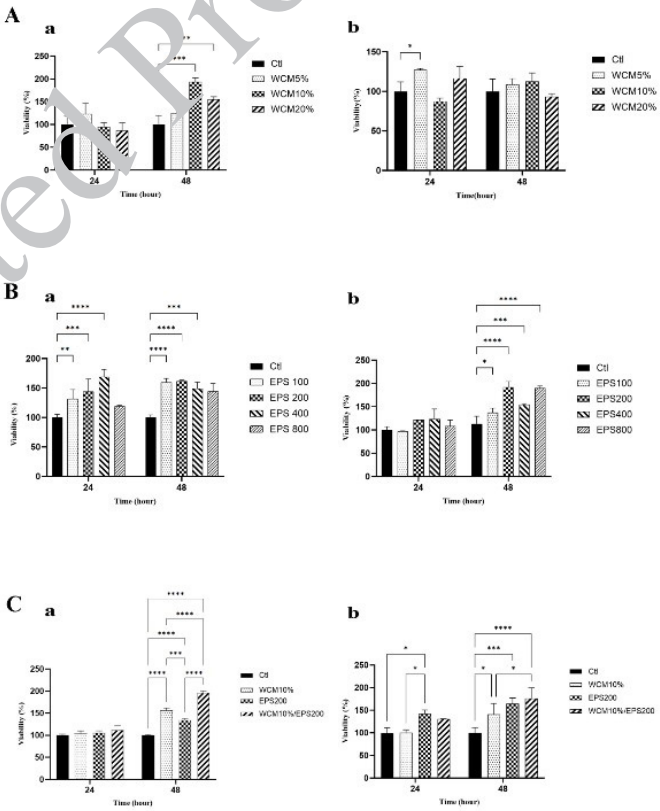

Figure 1. Cell viability (proliferation) of HFFs and HUVECs following rat treatment with WCM, EPS, or WCM/EPS, as determined by the MTT assay A) HFFs (Aa) and HUVECs (Ab) cultured for 24 and 48 hr in complete medium containing different concentrations of WCM (5%, 10%, and 20%; WCM5%, WCM10%, and WCM20%, respectively). B) HFFs (Ba) and HUVECs (Bb) cultured for 24 and 48 hr in complete medium containing different concentrations of EPS (100–800 µg/ml; EPS100–EPS800, respectively). C) HFFs (Ca) and HUVECs (Cb) cultured for 24 and 48 hr in complete medium containing WCM10%, EPS200, or WCM10%/EPS200. Control cells received complete medium without treatment. Data are presented as mean±SD (n=3). $P<0.05$.
HFFs: Human foreskin fibroblasts; HUVECs: Human umbilical vein endothelial cells; WCM: Wharton's jelly-derived mesenchymal stem cell-conditioned medium; EPS: Exopolysaccharide; Ctl: Control; MTT: 3-[4.5 dimethylthiazol- 2-yl]-2.5-diphenyltetrazolium bromide

Corrected Proof

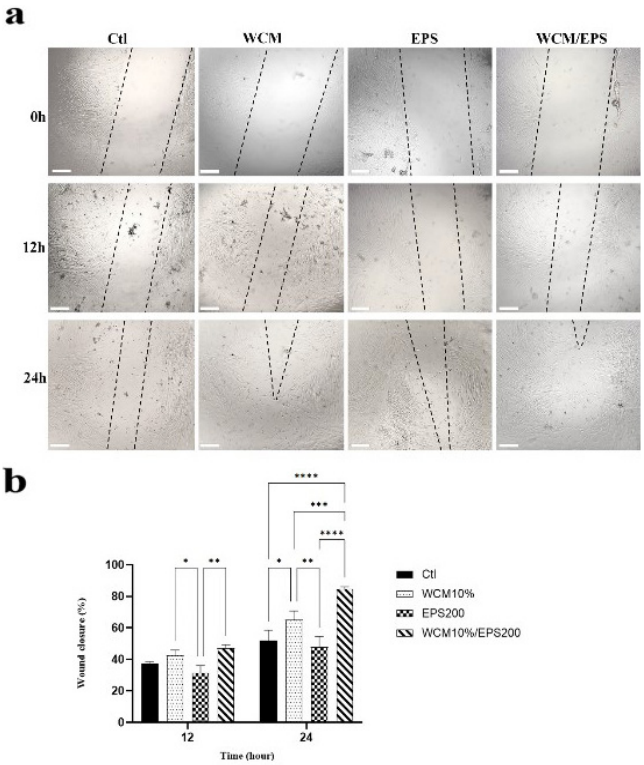

Figure 2. Scratch wound assay of HFFs following rat treatment with WCM, EPS, or WCM/EPS

a) Representative inverted microscope images showing the wound margins (dashed lines) at 0, 12, and 24 hr after scratching. b) Percentage of wound closure under the different treatment conditions. Control cells received complete medium without treatment. Data are presented as mean±SD (n=3). $P<0.05$.

HFFs: Human foreskin fibroblasts; WCM: Wharton's jelly-derived mesenchymal stem cell-conditioned medium; EPS: Exopolysaccharide; Ctl: Control

control group (Figure 1B). These results indicate that EPS promotes the proliferation of HFFs and HUVECs. Based on these findings, 200 µg/ml was selected as the optimal EPS concentration for subsequent *in vitro* and *in vivo* experiments. HFFs and HUVECs were then treated with the optimized EPS concentration (200 µg/ml), 10% WCM, or their combination (WCM/EPS). The MTT assay demonstrated that WCM/EPS exerted a greater proliferative effect on HFFs than either WCM or EPS alone (Figure 1C). These findings indicate that the WCM/EPS combination enhances HFF proliferation. In contrast, no significant difference in the proliferative effect on HUVECs was observed between the WCM/EPS and EPS groups (Figure 1Cb).

WCM/EPS augments wound closure

To investigate the effects of WCM, EPS, and WCM/EPS on the migration of HFFs and HUVECs, a scratch assay was used as an *in vitro* wound closure model. The results showed that 24 hr after scratching, the wound margins of HFFs treated with WCM and WCM/EPS were significantly closer together than those of the control group. No significant difference was observed between the EPS-treated and control groups (Figure 2a). The wound margins in the WCM/EPS-treated group nearly converged within 24 hr and were significantly closer than those in the WCM-treated group (Figure 2b). A scratch assay was also performed on HUVECs treated with WCM, EPS, WCM/EPS, and the control medium. The results showed that 24 hr after scratching, the wound edges of HUVECs treated with WCM and WCM/EPS had completely converged, and the scratched area was fully covered by migrating cells. In contrast, the wound edges in both the EPS-treated and control groups remained separated, leaving a considerable gap between them (Figure 3a). Statistical analysis further demonstrated that treatment with WCM and WCM/EPS significantly increased HUVEC migration compared with the control group. However, no significant difference was observed between the WCM and WCM/EPS groups. Likewise, HUVEC migration in the EPS treated group did not differ significantly from that in the control group (Figure 3b).

Gene expression

For this experiment, HFFs and HUVECs were treated with WCM, EPS, or WCM/EPS for 48 hr. Subsequently, the expression levels of the type I collagen and CDK4 genes in HFFs, and the VEGF-A gene in HUVECs, were evaluated. Statistical analysis revealed a relative increase in type I collagen gene expression in the WCM, EPS, and WCM/EPS groups compared with the control group; however, this difference was not statistically significant (Figure 4a). In contrast, CDK4 gene expression was significantly increased in the WCM, EPS, and WCM/EPS groups compared with the control group (Figure 4b). These findings are consistent with the MTT assay results obtained for HFFs treated with WCM, EPS, and WCM/EPS (Figure 1Ca). Furthermore, HUVECs treated with WCM, EPS, and WCM/EPS exhibited significantly higher VEGF-A expression than the control group (Figure 4c).

In vivo wound healing evaluation

Evaluation of the wound closure rate

Wound closure was evaluated by measuring the percentage reduction in wound area on days 0, 4, 9, and 14 (Figure 5a). Wound areas in all groups were quantified using

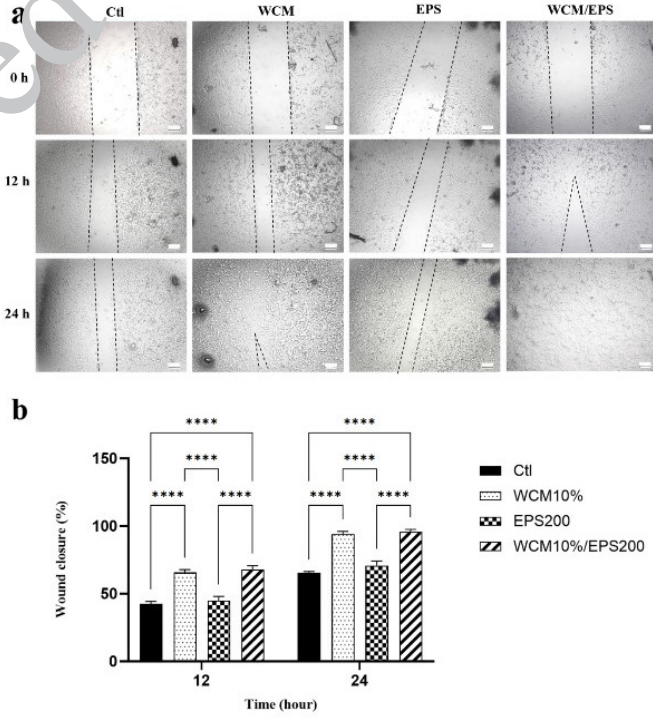

Figure 3. Scratch wound assay of HUVECs following rat treatment with WCM, EPS, or WCM/EPS

a) Representative inverted microscope images showing the wound margins (dashed lines) at 0, 12, and 24 hr after scratching. b) Percentage of wound closure under the different treatment conditions. Control cells received complete medium without treatment. Data are presented as mean±SD (n=3). $P<0.05$.

WCM: Wharton's jelly-derived mesenchymal stem cell-conditioned medium; EPS: Exopolysaccharide; Ctl: Control

Corrected Proof

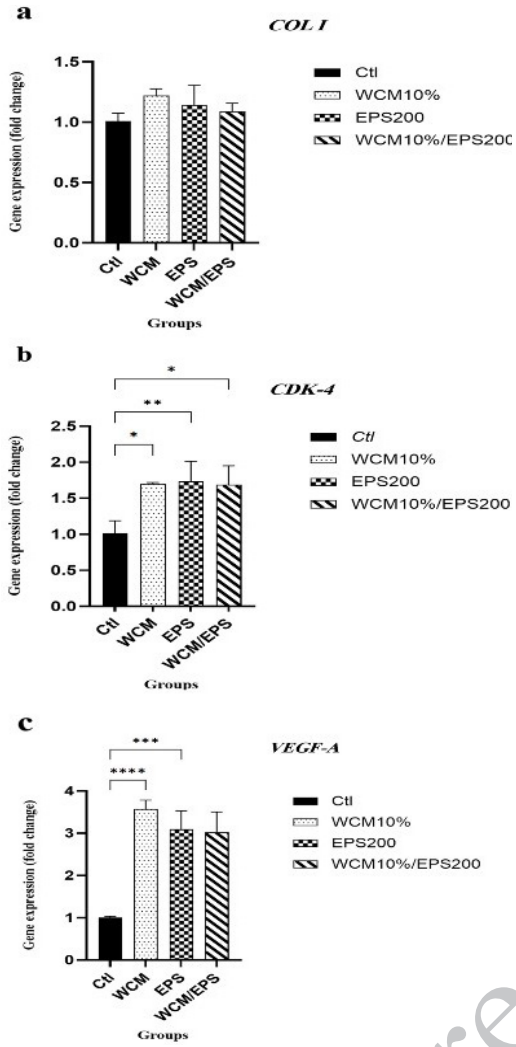

Figure 4. Quantitative RT-PCR analysis of rat gene expression following treatment with WCM, EPS, or WCM/EPS for 48 hr

a) Collagen type I (COL I) and b) CDK4 expression in HFFs, c) VEGF-A expression in HUVECs. Control cells received complete medium without treatment. Data are presented as mean±SD (n=3). $P<0.05$.

RT-PCR: Real-time PCR; HFFs: Human foreskin fibroblasts; HUVECs: Human umbilical vein endothelial cells; WCM: Wharton's jelly-derived mesenchymal stem cell-conditioned medium; EPS: Exopolysaccharide; Ctl: Control

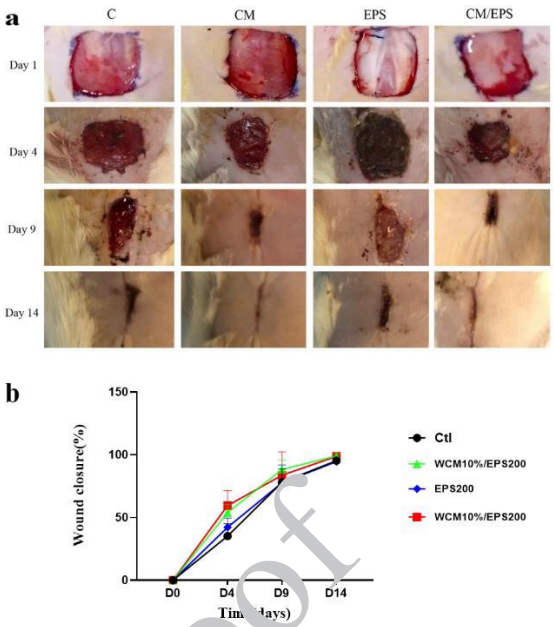

Figure 5. Rat wound closure following treatment with WCM, EPS, or WCM/EPS

a) Representative photographs of wounds on days 0, 4, 9, and 14 after wound creation in the different treatment groups. b) Percentage of wound closure in the different treatment groups. Data are presented as mean±SD.

WCM: Wharton's jelly-derived mesenchymal stem cell-conditioned medium; EPS: Exopolysaccharide; Ctl: Control

ImageJ software. During the observation period, the WCM and WCM/EPS groups showed greater wound closure than the control group, particularly in the early stages of wound healing (Figure 5b). By day 14, the WCM and WCM/EPS groups showed a higher percentage of wound closure than the control group (Figure 5b).

WCM/EPS improved histological parameters of diabetic wound healing

Histological examination on day 7 revealed no evidence of epidermal regeneration in the wound area of the control group. A large area of granulation tissue with a highly disorganized structure and marked infiltration of inflammatory cells, predominantly mononuclear cells such as lymphocytes and plasma cells, was observed (Figure 6a,

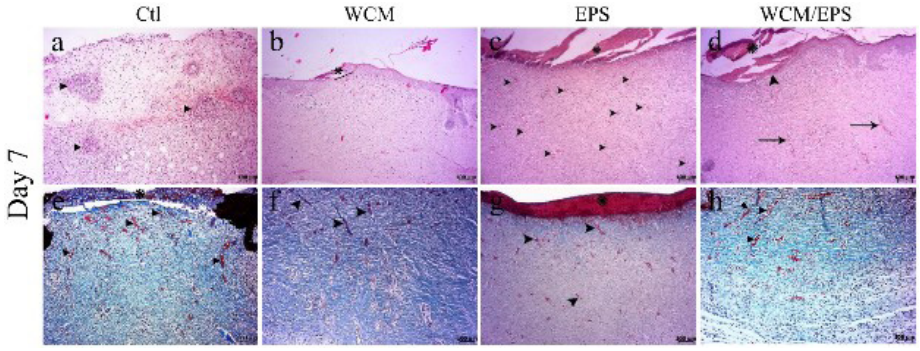

Figure 6. Representative photomicrographs of rat tissue sections stained with H&E and MT on day 7 after wound creation

a) Control (H&E): Extensive granulation tissue with infiltration of predominantly mononuclear inflammatory cells (arrowheads). b) WCM (H&E): Absence of newly formed epidermis at the wound surface (black line) with accumulations of necrotic tissue cells (*). c) EPS (H&E): Accumulations of fibrin strands, blood cells, neutrophils, and necrotic tissue cells on the wound surface (*), together with blood vessels oriented perpendicular to the wound surface (arrowheads) within the granulation tissue. d) WCM/EPS (H&E): Thin newly formed epidermis (arrowheads), with accumulations of neutrophils and necrotic tissue cells at the wound defect (*), and blood vessels oriented perpendicular to the wound surface (arrows). e) Control (MT): Blood vessels oriented perpendicular to the wound surface (arrowheads), together with accumulations of fibrin strands, blood cells, neutrophils, and necrotic tissue cells on the wound surface (*). f) WCM (MT): Granulation tissue with irregularly arranged connective tissue and blood vessels oriented perpendicular to the wound surface (arrowheads). g) EPS (MT): Accumulations of fibrin strands, blood cells, neutrophils, and necrotic tissue cells on the wound surface (*), together with blood vessels oriented perpendicular to the wound surface (arrowheads) within the granulation tissue. h) WCM/EPS (MT): Blood vessels oriented perpendicular to the wound surface (arrowheads).

H&E: Hematoxylin and eosin; MT: Masson's trichrome; WCM: Wharton's jelly-derived mesenchymal stem cell-conditioned medium; EPS: Exopolysaccharide

Corrected Proof

Table 1. Comparison of histopathological changes during wound healing among the rat experimental groups on days 7 and 14 after wound creation

Time	Groups	Re-epithelialization	Angiogenesis	Inflammatory cell infiltration	Bleeding	Edema	Organized granulation tissue
	Control	+	++++	++++	+++	+++	+
	CM	++	+++	+++	++	++	++
7th day	EPS	+	++++	+++	++	+++	+
	CM/EPS	+++	+++	++	++	++	+++
	Control	++	++++	++++	+++	+++	+
14th day	CM	+++	++	++	++	++	++
	EPS	++	+++	+++	++	++	+
	CM/EPS	++++	++	+	+	-	++++

Severity of histopathological changes: very low (+), low (++), moderate (+++), and high (++++).
CM: Conditioned medium; EPS: Exopolysaccharide; CM/EPS: Conditioned medium/exopolysaccharide

e). The severity of tissue damage was markedly reduced in the EPS, WCM, and WCM/EPS treatment groups compared with the control group. In the WCM/EPS group, the newly formed epidermis covered almost the entire wound surface (Figure 6d, h). In the WCM group, the epidermis covered most of the wound surface (Figure 6b, f), whereas in the EPS group, it was observed only at the wound margins (Figure 6c, g). Furthermore, the granulation tissue in the WCM/EPS group exhibited a more organized structure than that in the other groups. The control group showed the greatest inflammatory cell infiltration, followed by the EPS and WCM groups. In contrast, the WCM/EPS-treated group exhibited minimal inflammatory cell infiltration (Figure 6; Table 1). Histological examination on day 14 showed minimal epidermal regeneration over the wound surface in the control group. Instead, a large amount of irregularly organized granulation tissue was observed (Figure 7a), accompanied by marked infiltration of inflammatory cells (Table 1), predominantly mononuclear cells, including lymphocytes and plasma cells (Figure 7a). In the EPS group, epidermal tissue was observed only at the wound margins (Figure 7c, g). In the WCM group, the newly formed epidermis covered most of the wound surface but remained immature (Figure 7b, f). In the WCM/EPS group, the epidermis completely covered the wound surface and exhibited a more organized structure than that in the other treatment groups. In addition, a distinct stratum corneum was observed over the epidermal layer (Figure 7d, h). Furthermore, the granulation tissue in the WCM/EPS group was smaller and more organized than that in the EPS and WCM groups (Table 1). The control group exhibited the greatest inflammatory cell infiltration, followed by the EPS and WCM groups (Figure 7a; Table 1).

In contrast, the WCM/EPS-treated group exhibited minimal inflammatory cell infiltration. Assessment of blood vessel density at the wound site indicated that the WCM/EPS group had the lowest vessel density, followed by the WCM, EPS, and control groups (Figure 8a).

Table 1 summarizes the histopathological changes observed during wound healing in the experimental groups. Histological parameters, including re-epithelialization, inflammatory cell infiltration, hemorrhage, edema, and granulation tissue organization, were evaluated and scored by a veterinary pathologist. As shown in Table 1, the WCM/EPS-treated group had the most favorable histopathological scores across nearly all parameters.

Corrected Proof

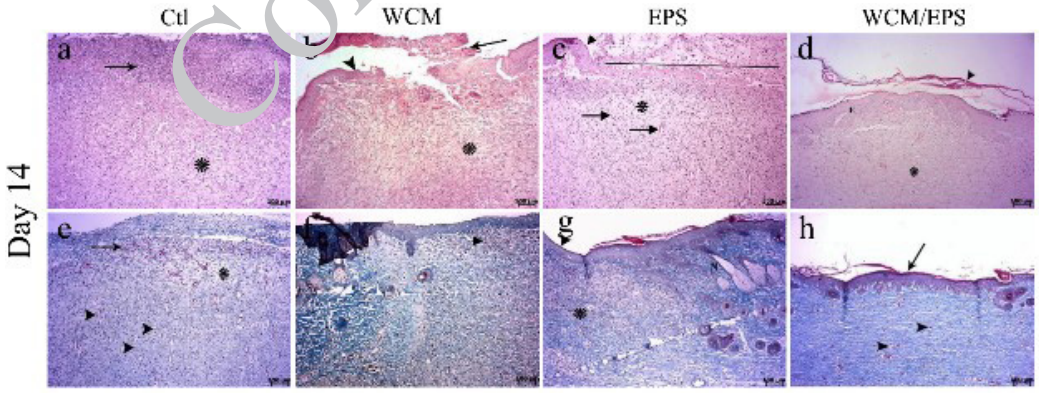

Figure 7. Representative photomicrographs of rat tissue sections stained with H&E and MT on day 14 after wound creation
a) Control (H&E): Severe infiltration of predominantly mononuclear inflammatory cells (arrow), with moderate interstitial edema (*) in the granulation tissue. b) WCM (H&E): Newly formed epidermis (arrowhead), small accumulations of neutrophils and necrotic tissue cells on the surface of the residual wound (arrow), and granulation tissue (*). c) EPS (H&E): Newly formed epidermis (arrowhead) at the wound edge (black line), with blood vessels oriented perpendicular to the wound surface (arrow) within the granulation tissue (*). d) WCM/EPS (H&E): Moderately thick epidermis covering the entire wound surface (E), together with the stratum corneum (arrowhead) and a small, well-organized granulation tissue (*). e) Control (MT): Blood vessels oriented perpendicular to the wound surface (arrowheads), moderate interstitial edema (*), and focal hemorrhage (arrow). f) WCM (MT): Slight focal hemorrhage beneath the epidermis (arrowhead) in granulation tissue with a relatively well-organized cellular arrangement. g) EPS (MT): Newly formed epidermis (arrowheads) at the wound edge (black line), granulation tissue (*), and normal skin tissue (N). h) WCM/EPS (MT): Epidermis with a well-developed stratum corneum (arrow), blood vessels with round cross-sectional profiles (arrowheads), and blue collagen fibers oriented parallel to the wound surface within the granulation tissue.
H&E: Hematoxylin and eosin; MT: Masson's trichrome; WCM: Wharton's jelly-derived mesenchymal stem cell-conditioned medium; EPS: Exopolysaccharide

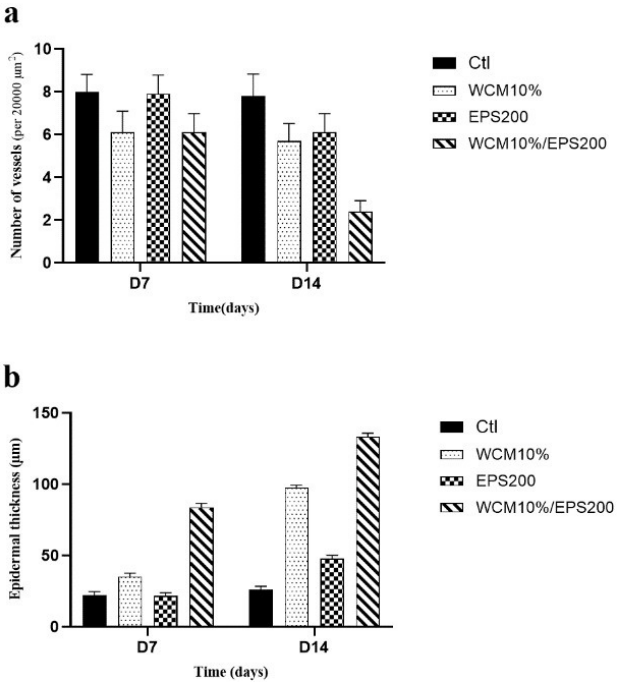

Figure 8. Histological assessment of rat blood vessel numbers and newly formed epidermis thickness on days 7 and 14 after wound creation
a) Number of blood vessels in the different treatment groups. b) Thickness of the newly formed epidermis in the different treatment groups. Data are presented as mean±SD.
Ctl: Control; WCM: Wharton's jelly-derived mesenchymal stem cell-conditioned medium; EPS: Exopolysaccharide

Discussion

Despite the availability of multiple therapeutic approaches, the management of DFU remains a significant challenge associated with diabetes. One promising strategy to address wound healing is to harness the therapeutic potential of mesenchymal stem cells (21-23). It has been demonstrated that the main therapeutic mechanism of MSCs is through paracrine signaling and the release of bioactive secretory factors (24).

The use of MSCs-CM may offer several advantages over living cells in terms of production, handling, maintenance, and product shelf life (25). Recent studies indicate that MSCs-CM enhances the survival, proliferation, and migration of fibroblasts, keratinocytes, and endothelial cells, thereby accelerating the wound healing process (26-28). In addition, Hivechi *et al.* (9) combined EPS-GUMS16 with polycaprolactone and gelatin to fabricate nanofibrous scaffolds for the treatment of full-thickness incisional wounds. Their study was the first to demonstrate the beneficial effects of EPS-GUMS16 on wound healing (9). However, this study investigated the effects of WCM/EPS on the behavior of fibroblasts and endothelial cells, two critical components of the wound-healing process. Compared with adult mesenchymal stem cells, such as bone marrow-derived mesenchymal stem cells (BM-MSCs), WJ-MSCs offer several advantages. These cells can be readily isolated from the umbilical cord, which is widely available and generally considered medical waste, using a non-invasive isolation procedure. Furthermore, recent studies have shown that wound healing-related factors, including FGF2, NGF, SDF-1, and HGF, are present at higher concentrations in the secretome of WJ-MSCs than in that of BM-MSCs (29).

We investigated the effects of EPS, WCM, and their combination (WCM/EPS) on the viability/proliferation and migration of fibroblasts and endothelial cells *in vitro*. Our findings, consistent with previous studies demonstrating the beneficial effects of WCM on fibroblast behavior (30), showed that EPS, both alone and in combination with WCM, enhanced fibroblast viability and proliferation. Moreover, the combined treatment promoted fibroblast proliferation more effectively than either treatment alone. Furthermore, although EPS alone did not significantly affect fibroblast migration, its combination with WCM promoted fibroblast migration more effectively than WCM alone. We further examined the effects of EPS, WCM, and their combination (WCM/EPS) on collagen type I expression in fibroblasts. The results showed no significant differences in collagen type I expression compared with the control group. Although collagen deposition is generally considered beneficial during wound healing, reducing it may be desirable in wounds prone to excessive scar formation. Our study also demonstrated that EPS enhanced endothelial cell proliferation; however, it did not significantly affect their migration compared with the control group. Furthermore, the combination of EPS and WCM did not produce a greater effect than WCM alone.

The proliferative effects of EPS on HFFs and HUVECs observed in the present study are consistent with the findings of Sahana and Rekha (31), who investigated the effects of an EPS derived from the bacterium *Alteromonas* sp. PRIM28 on fibroblast proliferation. Likewise, the absence of a significant effect of EPS, either alone or in combination with WCM, on HUVEC migration in our study is consistent with the findings of Matou *et al.* (32), who evaluated the effects of an EPS derived from Alteromonas infernus on HUVEC migration, both alone and in combination with FGF2 and VEGF. Nevertheless, they demonstrated that EPS sulfation significantly enhances its positive effect on HUVEC proliferation, both alone and in combination with FGF2 and VEGF. Specifically, they reported that sulfated EPS, when combined with FGF2 and VEGF, exerts a synergistic effect on HUVEC proliferation. In another study, Li *et al.*(33) suggested that the beneficial effects of polysaccharides derived from *Eucommia ulmoides* may be attributed to their interaction with FGF2 and PDGF-BB. Cell proliferation and migration during wound healing are stimulated by growth factors such as FGF, VEGF, KGF, and TGF-β. These growth factors activate signaling pathways, including MAPK/ERK and PI3K/PTEN/Akt, ultimately promoting cellular proliferation and migration (34, 35). Owing to the presence of various functional groups, including uronic acid residues, amino, sulfate, and phosphate groups, EPSs can engage in electrostatic interactions with chemokines and growth factors, thereby activating cellular signaling pathways (36). Owing to their structural similarity to the glycan components of the extracellular matrix, which serves as a reservoir for growth factors and facilitates their binding to cell surface receptors, EPSs are likely involved in activating specific cellular signaling pathways. This activation subsequently stimulates cellular proliferation and migration, thereby contributing to wound healing (37, 38). Additionally, owing to their structural characteristics and functional groups, some EPSs can interact directly with the cell membrane and may activate specific intracellular signaling pathways (39, 40). The helical and random-coil conformations of EPSs also play a significant role in their biological activity. For instance, owing to its helical conformation, β-glucan

Corrected Proof

can bind to multiple cell surface receptors and initiate intracellular signaling (41). The findings of our study, together with the evidence from the aforementioned studies, suggest that the enhanced proliferative effect of the WCM/EPS combination on HFFs is likely attributable to interactions between the growth factors present in WCM and EPS. Such interactions may enhance the accessibility of these growth factors to their corresponding cell surface receptors, thereby activating signaling pathways, such as MAPK/ERK, that promote cellular proliferation. In addition, the stimulatory effect of EPS on the proliferation of HFFs and HUVECs suggests that, given the presence of β-D-glucan chains in its structure(8), EPS may also directly bind to specific cell surface receptors and activate signaling pathways involved in cellular proliferation. The evaluation of the effects of EPS and WCM/EPS on endothelial cells revealed that WCM/EPS increased VEGF-A gene expression by approximately threefold compared with the control group, indicating its pro-angiogenic potential. Overall, our findings demonstrated that WCM/EPS enhanced fibroblast proliferation and migration more effectively than either treatment alone. Although EPS, both alone and in combination with WCM, positively affected endothelial cell proliferation and VEGF-A gene expression, the combined treatment did not produce additional improvements beyond those observed with WCM alone.

Although the combined WCM/EPS treatment consistently showed enhanced therapeutic efficacy across multiple experimental endpoints, the current study was not designed to distinguish additive from synergistic biological effects formally. Consequently, the mechanistic interpretations presented here should be viewed as hypothesis-driven explanations of complementary biological actions rather than definitive evidence of synergy.

Histological examination performed seven days after wound creation showed that, among the treatment groups, the WCM/EPS group exhibited nearly complete re-epithelialization across the entire wound surface. In contrast, the WCM and EPS groups showed incomplete re-epithelialization compared with the WCM/EPS group.

Specifically, in the WCM group, a new epidermal layer covered most of the wound surface, whereas in the EPS group, re-epithelialization was limited to the wound edges. Fourteen days after wound creation, the WCM/EPS-treated group exhibited complete wound coverage by a newly formed epidermis, including a well-developed stratum corneum, with the most organized epidermal architecture among the treatment groups. Histological evaluation indicated that the newly formed epidermis appeared thicker in the WCM/EPS group than in the WCM, EPS, and control groups. These findings suggest that the enhanced re-epithelialization observed in the WCM/EPS group may reflect improved keratinocyte proliferation and migration compared with the monotherapy groups.

Several studies, consistent with our findings, have reported that MSCs-CM (42, 43) and certain exopolysaccharides (31, 44) promote keratinocyte proliferation and migration. Recent studies have also shown that certain compounds with structures similar to exopolysaccharides can enhance the therapeutic effects of MSCs-CM (45, 46). As discussed above, EPS likely interacts with specific growth factors and cytokines present in WCM, thereby enhancing their accessibility to cell surface receptors and stimulating signaling pathways involved in cellular proliferation and migration. Furthermore, EPS may also directly bind to specific keratinocyte cell surface receptors, thereby potentiating the effects of WCM on cellular proliferation and migration. In the WCM/EPS group, the granulation tissue was smaller and more organized than that observed in the WCM and EPS groups, which may reflect the enhanced beneficial effects of the combined WCM/EPS treatment on fibroblast activity within the dermal layer.

Additionally, our results demonstrated that the WCM/EPS-treated group exhibited the lowest levels of inflammatory cell infiltration, edema, and hemorrhage, which may be attributed to the complementary biological effects of EPS and WCM. These histopathological findings collectively suggest that the combined WCM/EPS treatment promoted a transition of the diabetic wound microenvironment from a persistent inflammatory state toward a more regenerative tissue milieu. The marked reduction in inflammatory cell infiltration, edema, and hemorrhage likely facilitated the progression from the inflammatory phase to the proliferative phase of wound healing, thereby creating conditions favorable for re-epithelialization and granulation tissue maturation. Considering the previously demonstrated antioxidant properties of EPS-GLMS16, together with the immunomodulatory and regenerative activities of WCM-derived bioactive factors, these complementary biological actions may have contributed to the restoration of a tissue microenvironment more permissive to coordinated tissue repair and remodeling.

A reduction in the number of blood vessels within newly formed granulation tissue is considered one of the indicators of wound healing (47, 48). Histological evaluation indicated that the WCM/EPS-treated group exhibited a lower blood vessel density than the WCM- and EPS-treated groups, which may reflect a more advanced stage of granulation tissue maturation and wound healing following the combined treatment.

A limitation of the present study is the relatively small number of animals included in the histopathological evaluation at each time point. Because wounds within the same animal share the same systemic environment, the individual animal rather than the wound should be considered the appropriate biological unit of analysis. Therefore, the histological findings presented in this study should be interpreted with caution and treated primarily as descriptive observations. Future studies involving larger animal cohorts are warranted to validate these findings using adequately powered statistical analyses.

These findings further support the translational potential of the combined WCM/EPS therapy, highlighting its promise as a therapeutic strategy for diabetic wound healing and laying the foundation for future investigations into its clinical feasibility and applications. From a clinical perspective, both WCM and EPS are compatible with topical delivery systems, such as hydrogels (9, 49, 50) and sprays (51, 52), which are widely used in wound management because of their biocompatibility, ease of application, and ability to maintain a moist wound environment (53, 54). In the present study, the combination therapy was administered via localized periwound injection and topical spraying, thereby mimicking clinically relevant routes of administration and highlighting its potential for practical implementation. Scalability of production and cost-effectiveness are also important considerations for clinical translation. Exopolysaccharides derived from microbial

Corrected Proof

sources, such as Rhodotorula sp. GUMS16, used in the present study, is recognized for its high production yield, low manufacturing costs, and ease of downstream purification (55, 56). Likewise, WJ-MSCs represent a scalable, ethically acceptable, and non-invasive cell source, while the use of WCM eliminates the need for live cell transplantation, thereby reducing regulatory complexity (57, 58). Although combination biological therapies such as WCM/EPS may be subject to greater regulatory scrutiny, recent advances in regulatory frameworks for cell-free regenerative products and combination biologics by agencies such as the FDA and EMA have progressively clarified the developmental pathway for these therapies (59). Taken together, these considerations underscore the practical feasibility and future potential of this combination therapy. Nevertheless, further preclinical studies in large animal models that more closely resemble human physiology, together with long-term safety evaluations, are essential before clinical translation. Future studies should also focus on elucidating the biological mechanisms underlying the observed therapeutic effects. A better understanding of the mechanisms underlying the effects of EPS on cellular behavior, as well as the enhanced therapeutic effects of the combined WCM/EPS treatment on wound healing, requires further cellular and molecular investigations.

Additional molecular studies are warranted to clarify potential interactions between EPS and growth factors present in WCM, the signaling pathways involved in cellular proliferation and migration, and possible interactions between EPS and cell surface receptors.

Conclusion

In summary, WCM/EPS improved multiple wound healing parameters, including fibroblast proliferation and migration, re-epithelialization, inflammatory cell infiltration, granulation tissue organization, and edema. Across these parameters, the therapeutic effects of WCM/EPS were greater than those observed in the WCM, EPS, and control groups. These findings suggest that EPS enhances the therapeutic efficacy of WCM in diabetic wound healing. Therefore, the WCM/EPS combination represents a promising therapeutic candidate for treating diabetic wounds.

Acknowledgment

The results presented in this paper were part of a student's thesis. This study was funded by the School of Advanced Technologies in Medicine, Tehran University of Medical Sciences, Tehran, Iran (Research Project No. 1401-1-148-56967).

Authors' Contributions

H R handled conceptualization, drafted the original manuscript, and managed methodology, investigation, software, and data analysis. SMA H focused on software use, data analysis, data curation, and validation. N V contributed through review, editing, and supervision. S S and Z S were responsible for methodology development. PBM participated in conceptualization, review and editing of the manuscript, and supervision. J V contributed to conceptualization, project administration, review and editing, supervision, and secured funding.

Conflicts of Interest

The authors declare no competing interests.

Declaration

AI-assisted language-editing tools were used solely to improve the manuscript's English, grammar, and clarity. All scientific content, data analysis, interpretation of the results, and final decisions regarding the manuscript were made exclusively by the authors, who take full responsibility for the content of this work.

References

1. Alexiadou K, Doupis J. Management of diabetic foot ulcers. Diabetes Ther 2012;3:1-15.
2. Mieczkowski M, Mrozikiewicz-Rakowska B, Kowara M, Kleibert M, Czupryniak L. The problem of wound healing in diabetes—from molecular pathways to the design of an animal model. Int J Mol Sci 2023;23:7930.
3. Armstrong DG, Tan T-W, Boulton AJ, Bus SA. Diabetic foot ulcers: A review. JAMA 2023;330:62-75.
4. Aldana PC, Khachemoune A. Diabetic foot ulcers: Appraising standard of care and reviewing new trends in management. Am J Clin Dermatol 2020;21:255-264.
5. Hendrawan S, Marcelina O, Tan ST, Baer HU. Immobilization of hUC-MSCs conditioned medium on 3D PLLA collagen-coated matrix enhances diabetic wound healing progression. Eng Regen 2024;5:421-431.
6. Criollo-Mendoza MS, Contreras-Angulo LA, Leyva-López N, Gutiérrez-Grijalva EP, Jiménez-Ortega LA, Heredia JB. Wound healing properties of natural products: Mechanisms of action. Molecules 2023;28:598.
7. Sen S, Tiwari ON, Arya RK, Bhowmick TK, Gayen K. New insights on microbial extracellular polysaccharides: Production, biological activity, and applications. Biomass Conv Bioref 2025;15:24793-822.
8. Hamidi M, Gholipour AR, Delattre C, Sesdighi F, Seveiri RM, Pasdaran A, *et al.* Production, characterization and biological activities of exopolysaccharides from a new cold-adapted yeast: *Rhodotorula mucilaginosa* sp. GUMS16. Int J Biol Macromol 2020;151:268-277.
9. Hivechi A, Milan PB, Modabberi K, Amoupour M, Ebrahimzadeh K, Gholipour AR, *et al.* Synthesis and characterization of exopolysaccharide encapsulated PCL/gelatin skin substitute for full-thickness wound regeneration. Polymers 2021;13:854.
10. Huang Y-y, Wu J-m, Wu W-t, Lin J-w, Liang Y-t, Hong Z-z, *et al.* Structural, antioxidant, and immunomodulatory activities of an acidic exopolysaccharide from *Lactiplantibacillus plantarum* DMDL 9010. Front Nutr 2022;9:1073071.
11. Isildar B, Ozkan S, Koyuturk M. Therapeutic potential of mesenchymal stem cell-derived conditioned medium for diabetes mellitus and related complications. Adv Ther 2023;6:2300216.
12. Edwards SS, Zavala G, Prieto CP, Elliott M, Martínez S, Egana JT, *et al.* Functional analysis reveals angiogenic potential of human mesenchymal stem cells from Wharton's jelly in dermal regeneration. Angiogenesis 2014;17:851-866.
13. Yang Y, Huang Y, Yang J, Hu Z, Wu S, Yuan Q, *et al.* Umbilical cord mesenchymal stem cell-derived exosomes promote wound healing and skin regeneration via the regulation of inflammation and angiogenesis. Front Bioeng Biotechnol 2025;13:1641709.

Corrected Proof

14. Liang Y, Sun Q, Sun J, Xu M, Xu J, Yu Y. Adipose mesenchymal stem cells promote wound healing by modulating expression of SERPINE1 in dermal fibroblasts and keratinocytes. Stem Cells Int 2026;2026:5541440.
15. Rodrigues C, Paim TC, Zanatelli C, Prignon EVS, Azevedo JG, Naasani LIS, *et al.* Conditioned medium from human adipose-derived mesenchymal stromal cells can modulate cell migration and morphology of keratinocytes *in vitro*. Hum Cell 2026;39:42.
16. Zhao H, Song F, Ouyang L, Shi X, Shang S. Overexpression of IL-10 in adipose mesenchymal stem cells promotes wound healing in diabetic mice. Stem Cells Int 2026;2026:8861898.
17. Huang J, Beyer C, Palumbo-Zerr K, Zhang Y, Ramming A, Distler A, *et al.* Nintedanib inhibits fibroblast activation and ameliorates fibrosis in preclinical models of systemic sclerosis. Ann Rheum Dis 2016;75:883-890.
18. Sheehan DC, Hrapchak BB. Theory and Practice of Histotechnology. 2d ed. Mosby; 1980; P.101-120.
19. Therkildsen P, Haedersdal M, Lock-Andersen J, de Fine Olivarius F, Poulsen T, Wulf HC. Epidermal thickness measured by light microscopy: A methodological study. Skin Res Technol 1998;4:174-179.
20. Dominici M, Le Blanc K, Mueller I, Slaper-Cortenbach I, Marini F, Krause D, *et al.* Minimal criteria for defining multipotent mesenchymal stromal cells. The International Society for Cellular Therapy position statement. Cytotherapy 2006;8:315-317.
21. Gao M, Guo H, Dong X, Wang Z, Yang Z, Shang Q, *et al.* Regulation of inflammation during wound healing: the function of mesenchymal stem cells and strategies for therapeutic enhancement. Front Pharmacol 2024;15:1345779.
22. Xu J, Zgheib C, Hodges MM, Caskey RC, Hu J, Liechty KW. Mesenchymal stem cells correct impaired diabetic wound healing by decreasing ECM proteolysis. Physiological Genomics 2017;49:541-548.
23. Yu X, Liu P, Li Z, Zhang Z. Function and mechanism of mesenchymal stem cells in the healing of diabetic foot wounds. Front Endocrinol 2023;14:1099310.
24. da Silva Meirelles L, Fontes AM, Covas DT, Caplan AI. Mechanisms involved in the therapeutic properties of mesenchymal stem cells. Cytokine Growth Factor Rev 2009;20:419-427.
25. Vishnubhatla I, Corteling R, Stevanato L, Hicks C, Sinden J. The development of stem cell-derived exosomes as a cell-free regenerative medicine. J Circ Biomark 2014;3:2.
26. Liu C, Wang C, Yang F, Lu Y, Du P, Hu K, *et al.* The conditioned medium from mesenchymal stromal cells pretreated with proinflammatory cytokines promote fibroblasts migration and activation. PLoS One 2022;17:e0265049.
27. Sriramulu S, Banerjee A, Jothimani G, Pathak S. Conditioned medium from the human umbilical cord-mesenchymal stem cells stimulate the proliferation of human keratinocytes. J Basic Clin Physiol Pharmacol 2021;32:51-56.
28. Li S, Sun J, Yang J, Yang Y, Ding H, Yu B, *et al.* Gelatin methacryloyl (GelMA) loaded with concentrated hypoxic pretreated adipose-derived mesenchymal stem cells (ADSCs) conditioned medium promotes wound healing and vascular regeneration in aged skin. Biomater Res 2023;27:11.
29. Petrenko Y, Vackova I, Kekulova K, Chudickova M, Koci Z, Turnovcova K, *et al.* A comparative analysis of multipotent mesenchymal stromal cells derived from different sources, with a focus on neuroregenerative potential. Sci Rep 2020;10(1):4290.
30. Saheli M, Bayat M, Ganji R, Hendudari F, Kheirjou R, Pakzad M, *et al.* Human mesenchymal stem cells-conditioned medium improves diabetic wound healing mainly through modulating fibroblast behaviors. Arch Dermatol Res 2020;312:325-336.
31. Sahana T, Rekha P. A bioactive exopolysaccharide from marine bacteria *Alteromonas* sp. PRIM-28 and its role in cell proliferation and wound healing *in vitro*. Int J Biol Macromol 2019;131:10-18.
32. Matou S, Colliec-Jouault S, Galy-Fauroux I, Ratiskol J, Sinquin C, Guezennec J, *et al.* Effect of an oversulfated exopolysaccharide on angiogenesis induced by fibroblast growth factor-2 or vascular endothelial growth factor *in vitro*. Biochem Pharmacol 2005;69:751-759.
33. Li Q, Guo G, Meng F, Wang HH, Niu Y, Zhang Q, *et al.* A naturally derived, growth factor-binding polysaccharide for therapeutic angiogenesis. ACS Macro Lett 2016;5:617-621.
34. Welf ES, Haugh JM. Signaling pathways that control cell migration: models and analysis. Wiley Interdiscip Rev Syst Biol Med 2011;3:231-240.
35. Duronio RJ, Xiong Y. Signaling pathways that control cell proliferation. Cold Spring Harb Perspect Biol 2013;5:a008904.
36. Insulkar S, Kekar S, Lele S. Purification and structural-functional characterization of an exopolysaccharide from Bacillus licheniformis PASS26 with *in-vitro* antitumor and wound healing activities. Int J Biol Macromol 2018;110:1441-50.
37. Frantz C, Stewart KM, Weaver VM. The extracellular matrix at a glance. J Cell Sci 2010;123:4195-4200.
38. Senni K, Pereira J, Gueniche F, Delbarre-Ladrat C, Sinquin C, Ratiskol J, *et al.* Marine polysaccharides: A source of bioactive molecules for cell therapy and tissue engineering. Mar Drug 2011;9:1664-1681.
39. Dicker KT, Gurski LA, Pradhan-Bhatt S, Witt RL, Farach-Carson MC, Jia X. Hyaluronan: A simple polysaccharide with diverse biological functions. Acta Biomater 2014;10:1558-1570.
40. Péterszegi G, Isnard N, Robert A, Robert L. Studies on skin aging. Preparation and properties of fucose-rich oligo- and polysaccharides. Effect on fibroblast proliferation and survival. Biomed Pharmacother 2003;57:187-194.
41. Mundada PA, Mahajan HS. Pharmaceutical application of beta-glucan: A comprehensive overview. Futur J Pharm Sci 2025;11:77.
42. Li M, Zhao Y, Hao H, Dai H, Han Q, Tong C, *et al.* Mesenchymal stem cell–conditioned medium improves the proliferation and migration of keratinocytes in a diabetes-like microenvironment. Int J Low Extrem Wounds 2015;14:73-86.
43. Ademi H, Michalak-Micka K, Moehrlen U, Biedermann T, Klar AS. Effects of an adipose mesenchymal stem cell-derived conditioned medium and TGF-β1 on human keratinocytes *In vitro*. Int J Mol Sci 2023;24:14726.
44. Veeraperumal S, Qiu H-M, Zeng S-S, Yao W-Z, Wang B-P, Liu Y, *et al.* Polysaccharides from *Gracilaria lemaneiformis* promote the HaCaT keratinocytes wound healing by polarised and directional cell migration. Carbohydr Polym 2020;241:116310.
45. Humenik F, Danko J, Krešáková L, Vdoviaková K, Vrabec V, Vasilová E, *et al.* A Chitosan-Based biomaterial

Corrected Proof

combined with mesenchymal stem cell-conditioned medium for wound healing and skin regeneration. Int J Mol Sci 2023;24(22):16080.
46. Vidotti R, Yoshikawa A, Sant'Ana M, Souza H, Possebon L, da Rocha DN, *et al.* Reduction of inflammation and improvement of skin tissue repair using biomaterials composed of hydroxyapatite and chitosan associated to conditioned media derived from dental pulp stem cells. Int J Biol Macromol 2025;308:142353.
47. DiPietro LA. Angiogenesis and wound repair: When enough is enough. J Leukoc Biol 2016;100:979-984.
48. Fitridge R, Thompson M. Mechanisms of vascular disease: A reference book for vascular specialists: University of Adelaide Press; 2011.
49. Sendon-Lago J, Rio LG-d, Eiro N, Diaz-Rodriguez P, Avila L, Gonzalez LO, *et al.* Tailored hydrogels as delivery platforms for conditioned medium from mesenchymal stem cells in a model of acute colitis in mice. Pharmaceutics 2021;13:1127.
50. Nifontova G, Safaryan S, Khristidis Y, Smirnova O, Vosough M, Shpichka A, *et al.* Advancing wound healing by hydrogel-based dressings loaded with cell-conditioned medium: A systematic review. Stem Cell Res Ther 2024;15:371.
51. Park S-J, Hwang T, Jo S, Wooh S, Lee H, Jung Y, *et al.* Unveiling the diverse principles for developing sprayable hydrogels for biomedical applications. Biomacromolecules 2025;26:753-772.
52. Pleguezuelos-Beltrán P, Gálvez-Martín P, Nieto-García D, Marchal JA, López-Ruiz E. Advances in spray products for skin regeneration. Bioact Mater 2022;16:187-203.
53. Ho T-C, Chang C-C, Chan H-P, Chung T-W, Shu C-W, Chuang K-P, *et al.* Hydrogels: Properties and applications in biomedicine. Molecules 2022;27:2902.
54. Zhong G, Lei P, Guo P, Yang Q, Duan Y, Zhang J, *et al.* A Photo-induced Cross-Linking Enhanced A and B Combined multi-functional spray hydrogel instantly protects and promotes of irregular dynamic wound healing. Small 2024;20:2309568.
55. Okoro OV, Gholipour AR, Sedighi F, Shavandi A, Hamidi M. Optimization of Exopolysaccharide (EPS) Production by *Rhodotorula mucilaginosa* sp. GUMS16. ChemEngineering 2021;5:39.
56. Mouro C, Gomes AP, Gouveia IC. Microbial exopolysaccharides: Structure, diversity, applications, and future frontiers in sustainable functional materials. Polysaccharides 2024;5:241-287.
57. González-González A, García-Sánchez D, Dotta M, Rodríguez-Rey JC, Pérez-Campo FM. Mesenchymal stem cells secretome: The cornerstone of cell-free regenerative medicine. World J Stem Cells 2020;12:1529.
58. Smolinska V, Bohác M, Danišovič Ľ. Current status of the applications of conditioned media derived from mesenchymal stem cells for regenerative medicine. Physiol Res 2023;72:S233-S245.
59. Gupta DK, Tiwari A, Yadav Y, Soni P, Joshi M. Ensuring safety and efficacy in combination products: Regulatory challenges and best practices. Front Med Technol 2024;6:1371443.

Corrected Proof